Cell Stem Cell, Volume *12*

Supplemental Information

ROS Production and NF-κB Activation Triggered by RAC1 Facilitate WNT-Driven Intestinal Stem Cell Proliferation and Colorectal Cancer Initiation

Kevin B. Myant, Patrizia Cammareri, Ewan J. McGhee, Rachel A. Ridgway, David J. Huels, Julia B. Cordero, Sarah Schwitalla, Gabriela Kalna, Erin-Lee Ogg, Dimitris Athineos, Paul Timpson, Marcos Vidal, Graeme I. Murray, Florian R. Greten, Kurt I. Anderson, and Owen J. Sansom

Supplemental Inventory

Figure S1, Related to Figure 1

Figure S2, Related to Figure 2

Figure S3, Related to Figure 3

Figure S4, Related to Figure 4

Figure S5, Related to Figure 5

Figure S6, Related to Figure 6

Table S1, Related to Figure 2

Table S2, Related to Figure 2

Supplemental Experimental Procedures

Supplemental References

Figure S1, related to Figure 1.

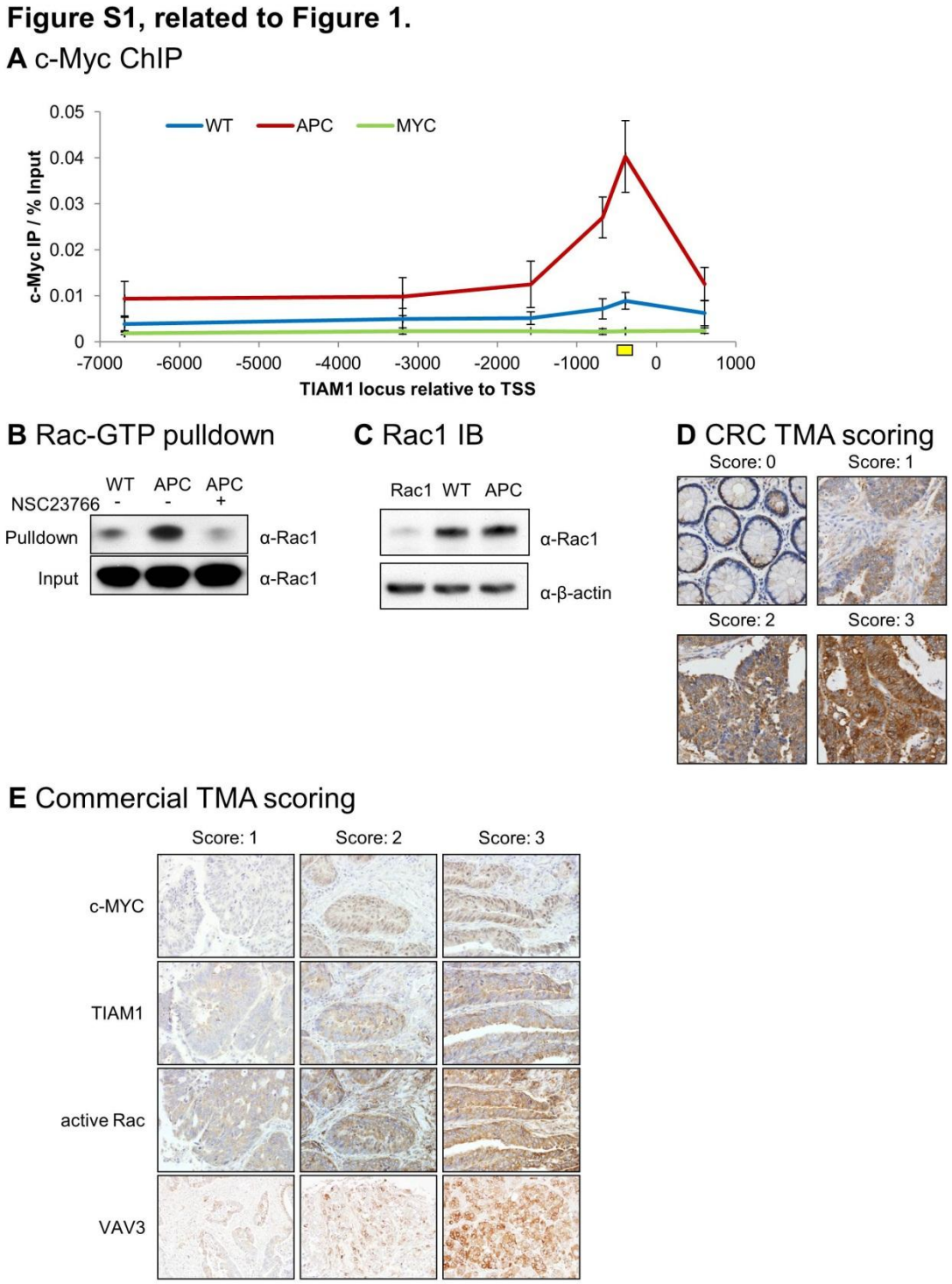

Figure S1, related to Figure 1. Rac1 activation following Apc loss. (A) ChIP of c-Myc to TIAM1 promoter performed on intestinal epithelial extractions from WT (blue line), APC (red line) and MYC (black line) deficient intestines. Error bars are SD. (B) Rac-GTP pulldown assays from WT, APC and APC mice treated with the Rac inhibitor NSC23766. (C) Immunoblotting total Rac1 levels in WT, APC and RAC1 deficient intestines. (D) Representative images of Rac-GTP staining intensities used for scoring prognostic human colorectal cancer TMA. (E) Representative images of staining intensities used for scoring colorectal cancer TMA.

Figure S2, related to Figure 2.

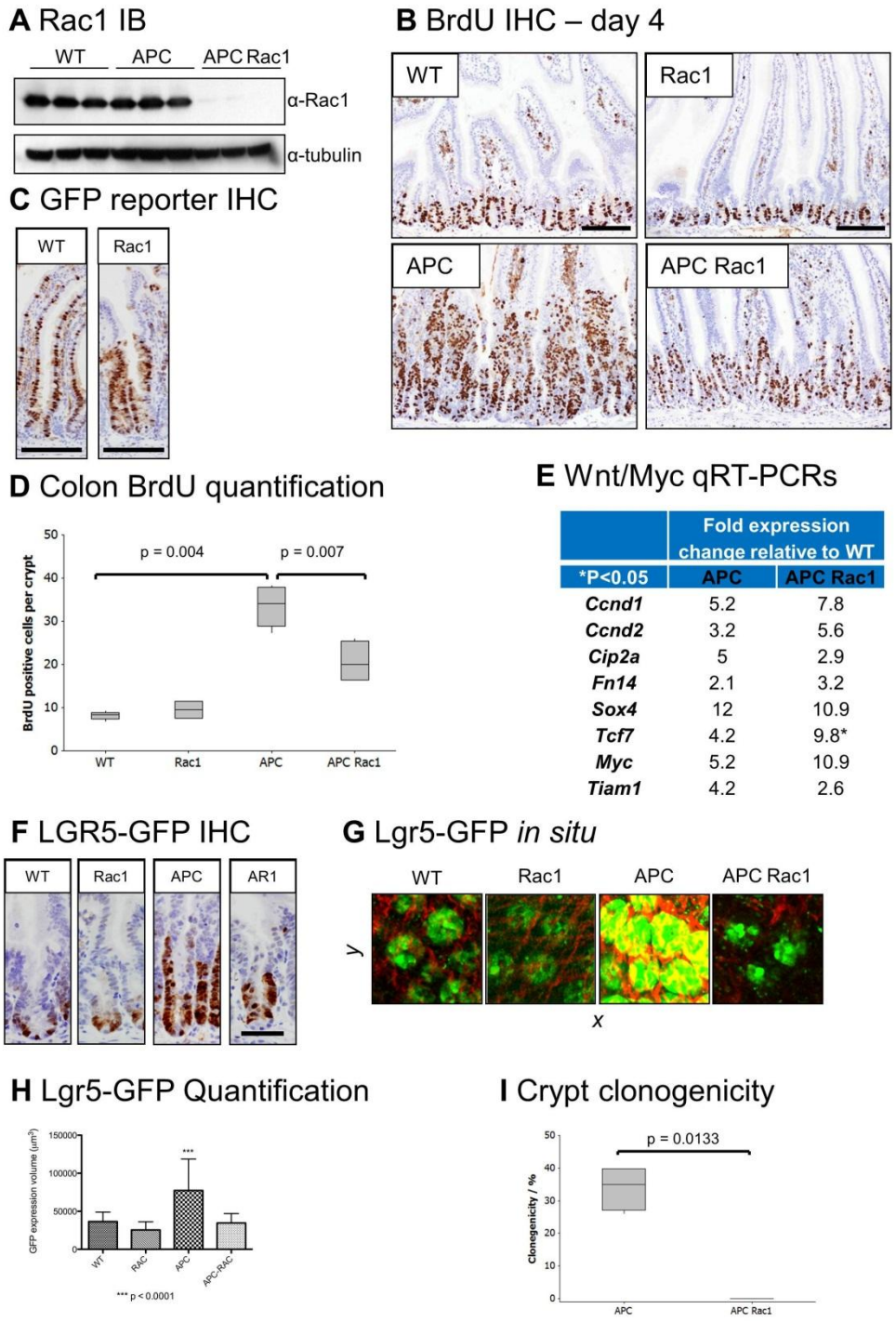

Figure S2, related to Figure 2. Phenotypic analysis of APC Rac1 co-deletion. (A) Confirmation of deletion of Rac1 in APC Rac1 mice. (B) BrdU IHC of intestines from WT, Rac1, APC and APC Rac1 mice. (C) IHC of GFP reporter expression in WT and Rac1 intestines 14 days post induction. Note GFP positive ribbons in both samples indicating stem cell function is intact. (D) Quantification of BrdU positivity shows a significant reduction of BrdU positivity in colons lacking Apc and Rac1 when compared to colons just lacking Apc (Mann Whitney, n=5). (E) QRT-PCR of selected TCF/LEF target genes within the intestinal epithelium. Fold change relative to WT control samples. Tcf7 is significantly upregulated in APC Rac1 intestine (Ttest, n=3, p=0.02). (F) GFP IHC of Lgr5-GFP expressing WT, Rac1, APC and APC Rac1

intestines. (G) Multiphoton microscopy analysis of Lgr5-GFP expression in WT, VilCreER Rac1, APC and APC Rac1. (H) Graph of crypt GFP expression volume (at least 50 crypts were scored across an average of 3 mice per genotype). Apc v Apc Rac1 (Error bars are SEM. Ttest, $p<0.0001$). (I) In vitro clonogenicity of APC and APC Rac1 crypts (Mann-Whitney, n=4). Scale bars correspond to 100µm.

Figure S3, related to Figure 3.

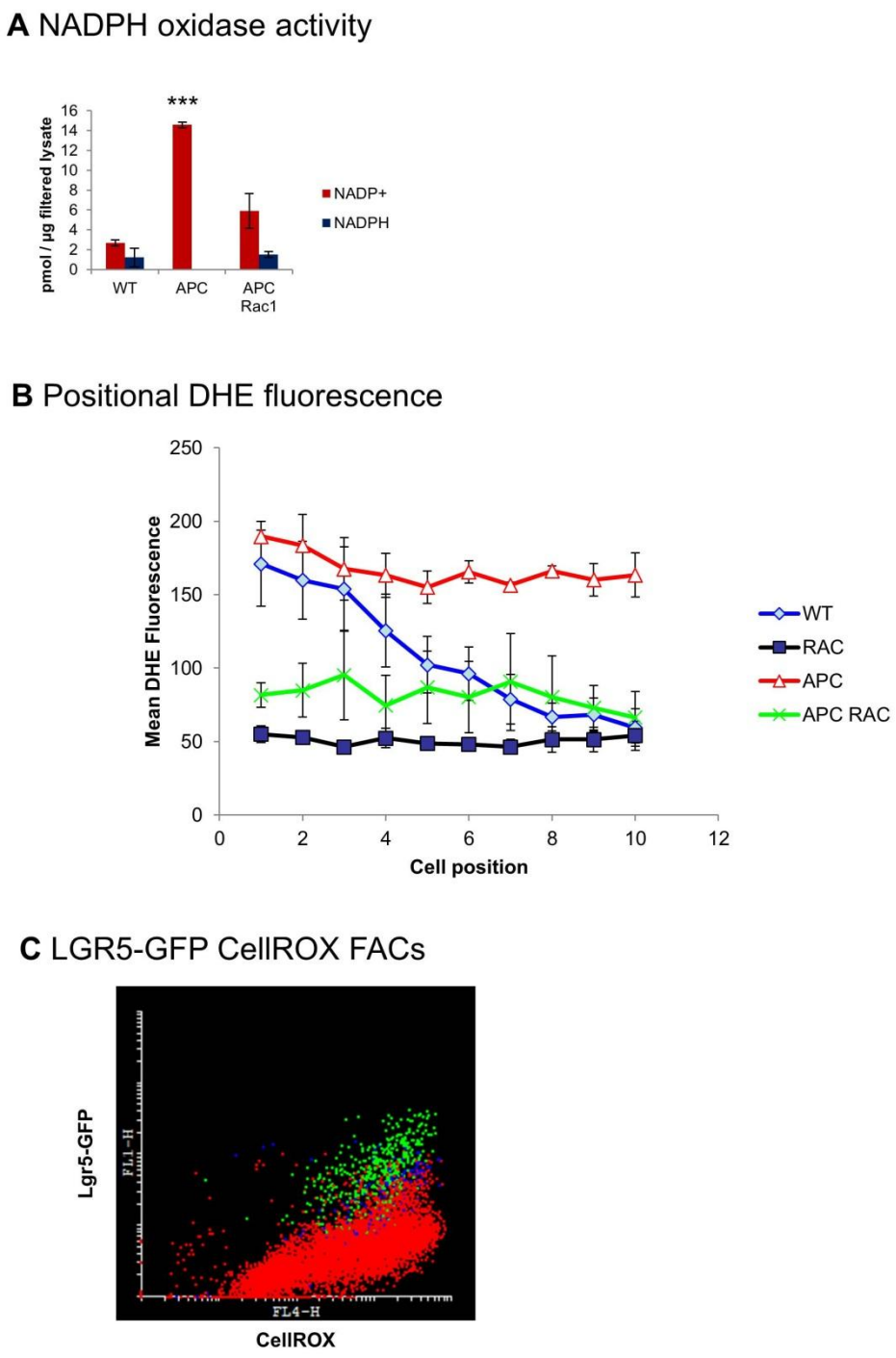

Figure S3, related to Figure 3. Rac1 is required for ROS production in the small intestine.

(A) Levels of NADP+ and NADPH in WT, APC and APC Rac1 intestines (Error bars are SD. Ttest, n=3, *** p<0.001, WT vs APC and APC vs APC Rac1). (B) Scoring of DHE fluorescence intensity based on cell crypt location. Error bars are SEM. (C) Histogram of CellROX intensity from all cells (blue line), *Lgr5*$^{GFP\text{-}CREER}$ +ve cells (green line) and *Lgr5*$^{GFP\text{-}CREER}$ -ve cells (red line).

Figure S4, related to Figure 4.

A qRT-PCR of Wnt target genes

	Fold expression change relative to WT	
*P<0.05	APC	APC + NAC
Ccnd1	20.4	15.2
Ccnd2	11.9	15.5
Fn14	22.2	15.2
Sox4	37.3	10.9*

B BrdU stain

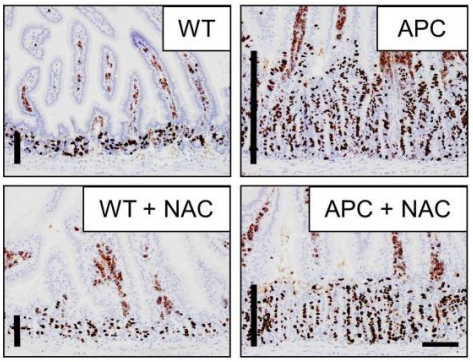

C qRT-PCR paraquat treated

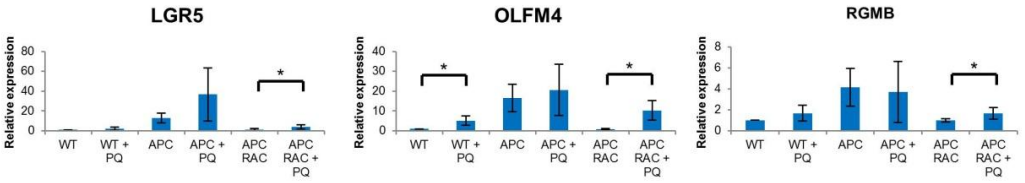

D Lgr5-GFP

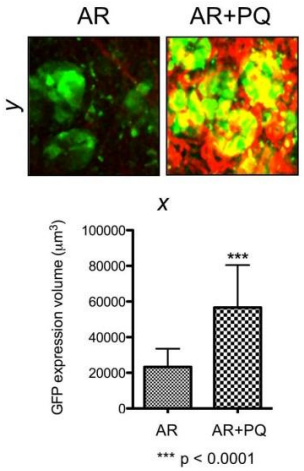

E BrdU paraquat treated

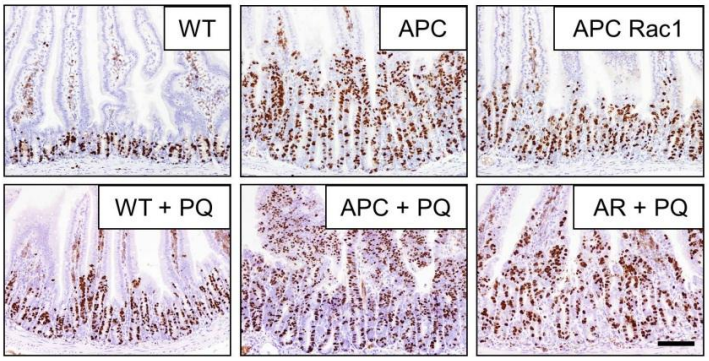

Figure S4, related to Figure 4. ROS is required for stem cells expansion in the small intestine.

(A) qRT-PCR of selected TCF/LEF target genes from intestines of APC and APC + NAC treated mice. Fold change relative to WT control samples. (B) BrdU staining of intestinal crypts from WT, APC, WT + NAC and APC + NAC mice. Vertical black bars denote crypt size. (C) qRT-PCR of 3 ISC markers, downregulated in APC Rac1 deficient intestines (AR) and upregulated upon treatment with paraquat (AR + PQ) (Error bars are SD. Ttest, n=3, * p<0.05, *** p<0.001). (D) *In situ* analysis of Lgr5-GFP expression in intestines from APC Rac1 and APC Rac1 mice treated with paraquat. Graph shows crypt volumes (Error bars are SEM. Ttest, p<0.0001). (E) BrdU IHC demonstrating increased proliferation in WT, APC and APC Rac1 mice following paraquat treatment.

Figure S5, related to Figure 5.

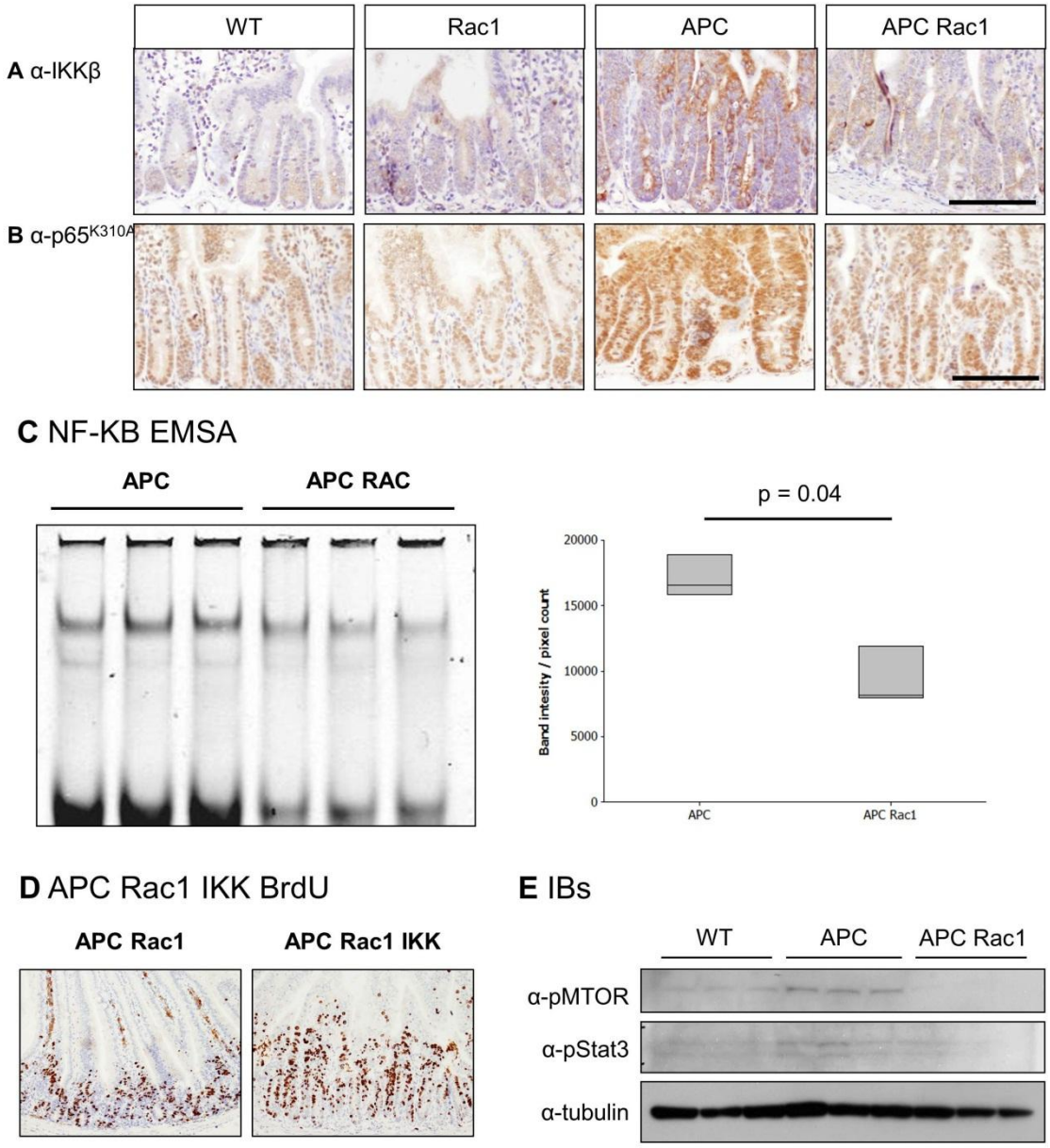

Figure S5, related to Figure 5. Activation of NF-κB signalling following APC loss requires Rac1. (A) IHC for IKKβ. Histoscoring identified a significant decrease in staining of APC Rac1 tissue compared to APC (p = 0.04, Mann Whitney, n-3). (B) IHC for the transcriptionally active, acetylated form of p65. Histoscoring identified a significant decrease in staining of APC Rac1 tissue compared to APC (p = 0.04, Mann Whitney, n-3). (C) EMSA analysis of binding to a NF-κB binding site probe of APC and APC Rac1 intestinal extracts. (D) BrdU staining of APC Rac1 and APC Rac1 IKK intestines. (E) IB of pMTOR and pStat3 from WT, APC and APC Rac1 deficient intestines. Scale bars correspond to 100μm.

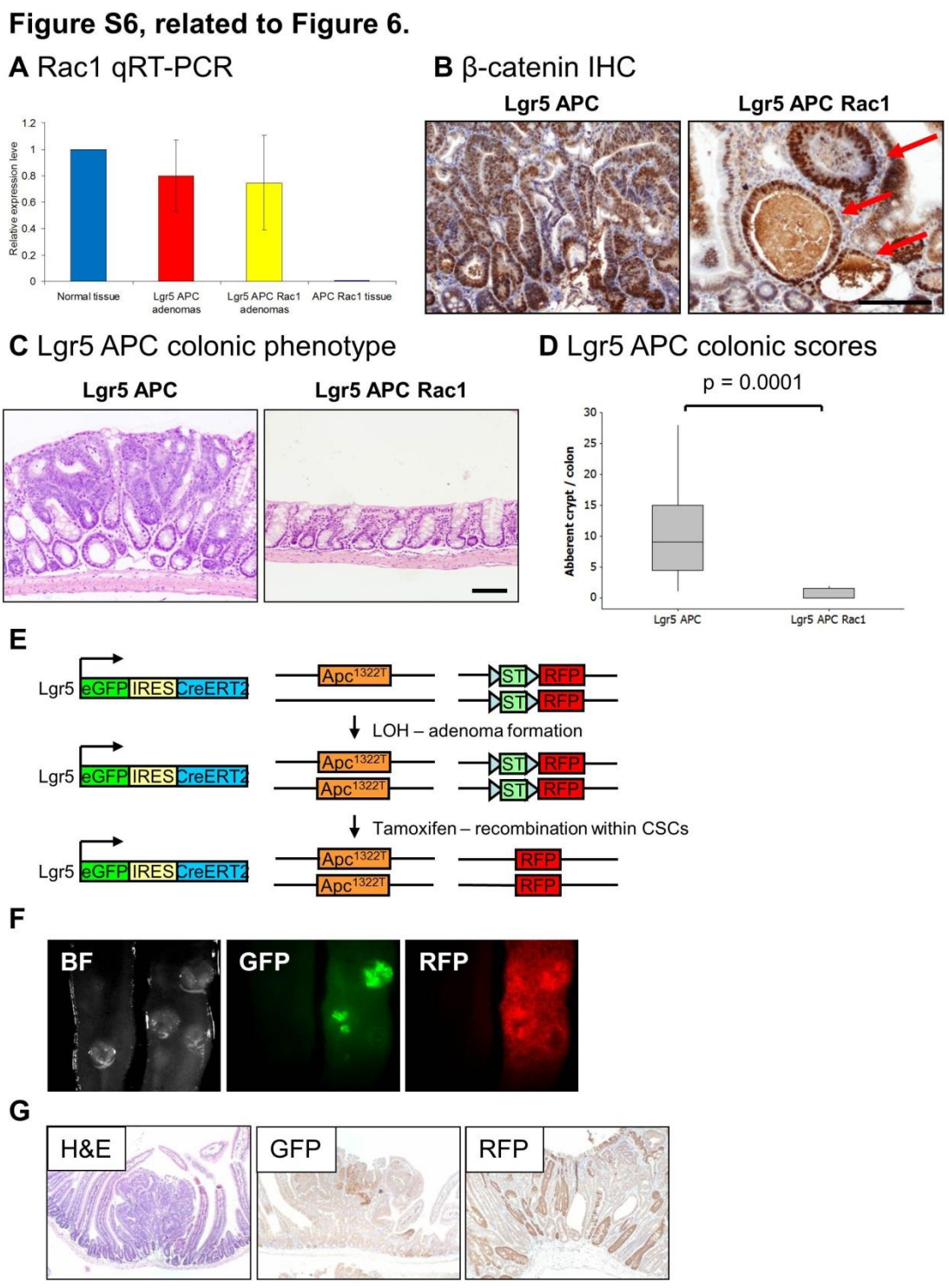

Figure S6, related to Figure 6. Characterisation of Lgr5 APC Rac1 model. (A) QRT-PCR examining levels of Rac1 in adenomas arising from Lgr5 APC and Lgr5 APC Rac1 mice. Adenomas do not have significantly different levels of Rac1 (Error bars are SD. Ttest, n=6, p=0.78). In contrast, there is a complete lack of Rac1 when QRT-PCR is performed in intestines following acute APC and Rac1 deletion. (B) IHC for β-catenin showing high levels of nuclear β-catenin in Lgr5 APC adenomas and within small lesions (red arrows) from Lgr5 APC Rac1 mice. (C) H&E staining of colonic lesions in Lgr5 APC mice compared to complete lack of lesions in Lgr5 APC Rac1 mice. (D) Scoring of lesion number identified histologically per

colonic section (Mann Whitney n ≥ 5). (E) Schematic outlining experimental procedure. (F) Wholemount analysis of tumours from *Apc*^{1322T} control (left) and *Apc*^{1322T} *Lgr5*$^{GFP\text{-}CREER}$ *Rosa26-RFP* (right) mice induced with tamoxifen for 4 days when showing signs of intestinal tumour burden. Note the strong Lgr5-GFP positivity in the tumours that corresponds to RFP positivity indicating that recombination has successfully occurred within the tumour. Images were taken using an Olympus OV100 microscope. (G) H&E stain of a typical adenoma from an *Apc*^{1322T} mouse (left). GFP staining of a tumour from an *Apc*^{1322T} *Lgr5*$^{GFP\text{-}CREER}$ mouse, note the areas of strong GFP positivity within the tumour (middle). RFP staining of a tumour from an *Apc*^{1322T} *Lgr5*$^{GFP\text{-}CREER}$ *Rosa26-RFP* mouse demonstrates recombination has occurred within the tumour (right).

Table S1, related to Figure 3. Step Up changes in expression.

(See accompanying Excel file.)

Table S2, related to Figure 3. Rank Product changes in expression.

(See accompanying Excel file.)

Supplemental Experimental Procedures

Intestinal epithelial extraction. To generate tissue for protein and RNA analysis gut epithelial tissue was extracted as previously described (Ayabe et al., 2000). Briefly, 10cm portions of intestine were flushed with PBS and inverted over a glass rod to expose the epithelial surface. Intestines were incubated in PBS + 30mM EDTA for 5 minutes followed by 30s of vigorous shaking for a total of 6 incubations. Microscopic analysis identified fractions 5 (20-25 min) and 6 (25-30 min) as containing predominantly crypts. These fractions were used for downstream analysis.

Primary antibodies. Primary antibodies and concentrations used for immunohistochemistry were as follows: β-catenin (1:50; Transduction Laboratories), BrdUrd (1:500; BD Biosciences), c-Myc (1:200; Santa Cruz sc-764), active-Rac (1:500; NewEast Biosciences 26903), Tiam1 (1:150; Santa Cruz sc-872), NF-κB p65 (1:100; Abcam ab7970), acetyl-p65 (1:100; Cell Signalling Technology 3045), IKKβ (1:100; Cell Signalling Technology 2678), GFP (1:1000; Abcam ab6556), RFP (1:500; Abcam ab34771), acetyl-p65 (1:100; Cell Signalling Technology 3045) and Vav3 (1:250; ab21208). Immunohistochemistry was performed on formalin-fixed intestinal sections.

Assaying proliferation in vivo. Proliferation levels were assessed by measuring bromodeoxyuridine (BrdU) incorporation. Mice were injected with 250 µl of BrdUrd (Amersham Biosciences) 2 hours before being sacrificed. Immunohistochemical staining for BrdUrd was then performed using an anti-BrdUrd antibody (1:500; BD Biosciences). At least three mice were used for each genotype.

Western blotting. Primary antibodies used for Western blotting were as follows: Rac1 (1:20000; CellBiolabs 240106), pMTOR (1:100; Cell Signalling Technology 2976), α-tubulin (1:20000; Sigma 6199) and pStat3 (1:500; sc-7993-R).

RNA isolation. RNA was isolated from epithelial extractions using a Qiagen RNeasy Mini Kit (Qiagen, Crawly, West Sussex, UK) according to the manufacturer's instructions. DNA-free (Ambion/Applied Biosystems, Warrington, UK) was used to remove genomic DNA contamination from the RNA prior to RT-PCR, according to the manufacturer's instructions.

Quantitative PCR (qPCR). 1ug of RNA was reverse transcribed to cDNA using a DyNAmo SYBR Green 2-step qPCR kit (Finnzymes, Espoo, Finland) in a reaction volume of 20ul. qPCR was performed in triplicate in a 20 µl reaction mixture containing 10 µl of 2 × DyNAmo HS master mix, 0.5 µM of each of the primers and 0.1 µl cDNA. The reaction mixture without a template was run as a control. The cycling conditions were as follows: 95°C for 15 min, followed by 40 cycles of three steps consisting of denaturation at 94°C for 15 s, primer annealing at the optimal temperature for 30s, and primer extension at 72°C for 30s. A melting curve analysis was performed from 70°C to 95°C in 0.3°C intervals

to demonstrate the specificity of each amplicon and to identify the formation of primer dimers. β-actin or Gapdh were used to normalize for differences in RNA input.

Active Rac binding assay. In vivo Rac activation was assessed using a Rac activation assay kit (Cellbiolabs), Wildtype or *VilCreER Apc*$^{fl/fl}$ mice were given daily 80mg/kg-tamoxifen IP injections for 4 days and culled 4 days after the first injection. Pieces of gut were isolated and lysed in the lysis buffer provided using a Precellys 24 tissue homogeniser. For NSC23766 treatment mice were IP injected with 4mg/kg NSC23766 on days 2, 3 and 4 following tamoxifen induction.

Colorectal cancer tissue microarray. A colorectal cancer tissue microarray was constructed containing normal colon mucosa (n=50), primary (n=650) and metastatic colorectal cancer (n=285). The metastases were all from tumour involved lymph nodes of the stage 3 (Dukes C) cases. Each normal sample was acquired from at least 10 cm distant from the tumour as previously described (Carpenter et al., 2006; Coghlin et al., 2006; Duncan et al., 2008; Hope and Murray, 2011; Kumarakulasingham et al., 2005; O'Dwyer et al., 2011). In total, tumour samples from 650 patients were involved in this study, in each case, a diagnosis of primary colorectal cancer had been made, and the patients had undergone elective surgery for primary colorectal cancer, in Aberdeen, between 1994 and 2009. Survival information was available for all patients and at the time of censoring patient outcome data there had been 309 (47.5%) deaths. The mean patient survival was 115 months (95% CI, 108-124 months). None of the patients had received any pre-operative chemotherapy or radiotherapy. The histopathology of each case was reviewed and areas of tissue to be sampled were first identified and marked on the appropriate haematoxylin and eosin stained slide by an expert consultant gastro-intestinal pathologist (GIM). Two 1mm cores were taken from these areas of the corresponding wax embedded block using a Beecher Instruments tissue microarrayer (Sun Prairie, WI, USA) and placed in a recipient paraffin block (O'Dwyer et al., 2011). Following transfer, the recipient array block was heated to 37^{o}C, and a glass slide was used to carefully press down the cores to ensure they were all at the same level within the recipient wax block. Sections (4 microns) in thickness were cut and mounted on coated slides for immunohistochemistry. Statistical analysis of the immunohistochemical data including Kaplan-Meier survival analysis, and log-rank test was performed using SPSSv19 for Windows XP™ (SPSS UK, Ltd, Woking, UK). The development of the colorectal cancer tissue microarray had the approval of The North of Scotland Research Ethics Committee (ref. nos. 08/S0801/81; 11/NS0015).

Commercial TMA. Colon carcinoma tissue arrays (CO804, Biomax.us) were stained with the following antibodies: c-Myc (1:200; Santa Cruz sc-764), active Rac (1:500; NewEast Biosciences 26903), Tiam1 (1:150; Santa Cruz sc-872) and Vav3 (1:250; ab21208). Individual cores were scored based on the percentage of each core with a staining intensity of 0, 1, 2 or 3. Staining intensities were analysed using the Spearman's rank correlation coefficient

Chromatin Immunoprecipitation (ChIP). For ChIP analysis crypts isolated by epithelial extraction were fixed with 1% formaldehyde for 10 mins at room temperature. The formaldehyde is quenched with 125mM glycine for 5 mins at room temperature. Samples were sonicated for 0.5 min on; 0.5 min off, 2 x 15 mins setting high. Sonicated samples were cleared by centrifugation at 13000rpm at 4C for 5 mins. Chromatin was immunoprecipitated overnight at 4C with the following antibodies: c-Myc (1:10; Santa Cruz sc-764), NF-κB p65 (1:10; Abcam ab7970), rabbit IgG control (1:10, DAKO P0449). IgG complexes were captured with 25ul of protein G dynabeads (Invitrogen) for 1h. Captured complexes were washed with 2 x 1ml Tiam1 buffer, 2 x 1ml LiCl buffer and 2 x 1ml TE. DNA was eluted overnight with 100ul TE, 1% SDS, 150mM NaCl, 5ul proteinase K at 65C. DNA was purified with Qiagen PCR purification kit and eluted with 100ul elution buffer. 5ul of DNA was used per qPCR reaction. Samples equating to 25% of input was also isolated and used in qPCR analysis. IP efficiency as a percentage of input was calculated based on DCt values obtained in qPCR reactions.

In vivo imaging of ISCs. Intestinal tissue explants were taken from Lgr5-GFP expressing mice and exposed to 50mg/ml (-)-scopolamine-N-butylbromide for 10 minutes to minimise peristalsis. All imaging was performed on a Nikon Eclipse TE2000-U inverted microscope with an Olympus long working distance 20x 0.95 NA water immersion lens. The excitation source used for all image acquisition was a Ti:Sapphire femto-second pulsed laser (Cameleon, Coherent UK). A scan head specifically designed for multi-photon excitation was used (Trim-scope, LaVision Biotec, Germany) to control all beam scanning and data acquisition. The Trim-scope multiphoton microscope was used to image regions of tissue measuring typically 2 x 2 mm composed of 500 x 500 x 100 µm regions. The excitation wavelength was 890 nm and a 435/40 nm band pass filter used to filter the SHG and a 525/50 nm band pass filter used for the GFP emission. A 500 nm LP dichroic was used to spectrally separate the emission signal. For optimal efficiency, the detectors were placed again in the NDD port at the back aperture of the objective lens. Xuv-tools GUI (Emmenlauer et al., 2009) was used post-acquisition to stitch together the component regions. The tiled regions were exported into Imaris (Bitplane) for 3-D reconstruction. Following 3-D reconstruction a solid surface was created based on GFP fluorescence. This defined the volume of GFP expression in the stem cell compartment of the individual crypt regions. The individual crypt volumes were exported into Excel for analysis. A minimum of 50 crypts from at least 3 mice of each genotype were analysed.

DHE staining on cryosections. OCT covered tissues were cut in 8µm sections. Slides were incubated at 37° C in 30µM DHE (Invitrogen Molecular Probes D11347) for 7 min. Vectashield containing DAPI (Vector Laboratories, Inc.) was used as counter stain. Samples were immediately analysed with a Zeiss 710 upright confocal microscope. Fluorescence intensity of at least 100 nuclei per sample was scored in at least 3 mice.

Crypt isolation and propagation. Mouse small intestines were opened longitudinally and washed with PBS. Crypts were isolated as previously described (Sato et al., 2009). 100 crypts, mixed with 50 µl of Matrigel (BD Bioscence) were plated in 24-well plates in Advanced DMEM/F12 with EGF (50 ng/ml, Peprotech) and Noggin (100 ng/ml, Peprotech). Growth factors were added every other day. Sphere formation was scored 7 days after plating. For transplantation experiments 100 just purified crypts were suspended in 100 µL Matrigel and injected s.c. into 6-week-old female athymic (CD1) mice.

FACS analysis. Mouse small intestines were opened longitudinally and washed with PBS. Adenomas were isolated, chopped into small pieces and washed with cold PBS. The tissue fragments were incubated with EDTA 5 mM in PBS for 10 min. After removal of EDTA, the tissue fragments were incubated with trypsin (2.5%) and 100 units DNase for 30 min at 37°C. The tissue fragments were vigorously suspended, diluted with Advanced DMEM/F12 medium and passed through a 40 µm strainer. For ROS analysis, cells were stained for 30min at 37C with 5uM CellROX Deep Red (Invitrogen Molecular Probes C10422). Cells were centrifuged at 300g for 5 min. $EpCAM^{+}/GFP^{+}$ and $EpCAM^{+}/GFP^{-}$ cells were sorted by flow cytometry. Single viable cells were gated by negative staining for DAPI.

GFP reporter lineage tracing. *AhCre* $Rac1^{fl/fl}$ mice were crossed to mice carrying a *RosaLoxStopLox-GFP* allele (Novak et al., 2000) to generate *AhCre* $Rac1^{fl/fl}$ *RosaLoxStopLox-GFP* and control *AhCre RosaLoxStopLox-GFP* mice. These were induced with a single IP injection of β-napthaflavone and sacrificed 14 days later. Lineage tracing capacity of Rac1 deficient ISCs was determined by GFP IHC.

NADP/NADPH assay. NADP+ and NADPH levels were measured from intestinal tissue using a NADP/NADPH Assay Kit (ab65349). WT, APC and APC Rac1 mice were induced with tamoxifen as described and culled 4 days later. 20mg of small intestinal tissue was lysed in the lysis buffer provided using a Precellys 24 tissue homogeniser. Lysates were cleared by centrifugation at 13,000rpm for 10 min and then filtered through 10 kDa molecular weight cut off filters (ab93349) before performing the assay. A standard curve time course was performed at 10 minute intervals to determine optimal incubation time (20 minutes at RT) for analysis. NADP and NADPH levels in total lysate were calculated by comparison to the standard curve. Protein concentration was determined for each samples and values represented as pmol NADP / NADPH per ug filtered lysate.

RT-PCR primers

Primer name	Primer sequence
Tiam1 F	TGCAGTTCCCCAGAGAGC
Tiam1 R	CACACAATCTCTTGCCTCCA

Olfm4 F	GCCACTTTCCAATTTCAC
Olfm4 R	GAGCCTCTTCTCATACAC
Rgmb F	GCTACACACTGGAGACTGCCA
Rgmb R	AGTTGGCATCACCAGTGGTGAG
Tcf7 F	CACCACAGGAGGAAAAAGAAATG
Tcf7 R	CAAGGAGGGCAACAGAAGATAC
Tnfrsf12a (Fn14) F	CTGGTTTCTAGTTTCCTGGT
Tnfrsf12a (Fn14) R	CTTGTGGTTGAAAGAGTCTG
Ccnd2 F	CTACCGACTTCAAGTTTGCC
Ccnd2 R	GCTTTGAGACAATCCACATCAG
Cdk4 F	AATGTTGTACGGCTGATGGA
Cdk4 R	AGAAACTGACGCATTAGATCCT
Ccnd1 F	GAGAAGTTGTGCATCTACACTG
Ccnd1 R	AAATGAACTTCACATCTGTGGC
Lgr5 F	GAGTCAACCCAAGCCTTAGTATCC
Lgr5 R	CATGGGACAAATGCAACTGAAG
Tnfrsf19 (Troy) F	CTGGATTTGAAGTTTGTCTG
Tnfrsf19 (Troy) R	CGTGTTTATTCCTGCTACTC
Myc F	TGAAGAAGAGCAAGAAGATGAG
Myc R	CTGGATAGTCCTTCCTTGTG
ActB F + R	Primer Design Control Set
Gapdh F + R	Primer Design Control Set
Cip2a F	GAACAGATAAGGAAAGAGTTG
Cip2a R	ACCTTCTAATTGAGCCTTGTG

Rac1 F	GAGACGGAGCTGTTGGTAAAA
Rac1 R	ATAGGCCCAGATTCACTGGTT
Rac1b F	TGTGGTAAAGATAGACCCTCC
Rac1b R	CCCACGAGGATGATAGGAGT
Vav3 F	AGAAACGGACCAATGGACTTC
Vav3 R	ATGGAGAGGGTTTGACAGCAT

ChIP primers

TIAM1 7kb up F	TGG GCC ATC ACC CTA TGC AAG AAA
TIAM1 7kb up R	AGA ATG GAG TGG AAG GGC TGG AAA
TIAM1 4kb up F	TAC CCT GTT AGA AGC TGC CGT GTT
TIAM1 4kb up R	ATA TGT GAG GGC TTG AGA CTG GCA
TIAM1 2kb up F	ACT CAG AGA CAG CTG CAT CAC CA
TIAM1 2kb up R	ACT TGG AAA GGA CAG GCT CCT ACA
TIAM1 1kb up F	TAT GTC TGG TGA CAG GCA GCT TCA
TIAM1 1kb up R	ACC GCA GCA AGA ATA ACG AGA CCT
TIAM1 1kb down	TTC GTG TGC ATA CAC TTG GGA GGT
TIAM1 1kb down R	TGT CAC TTG CAT TCG GCT CCA GTA
TIAM1 Ebox F1	ACC TAA AGT CTG TTT GGT GGC GGA
TIAM1 Ebox R1	TAC CTG CGA CAC GTG GTC TAG TTT
Lgr5 promoter F	ACCAGTGAGAGTGGGCAGAG
Lgr5 promoter R	CGCAGTCATGGTCTTTCTCA
Rgmb promoter F	TCGAGAAGTCAGTAGGGCAGA
Rgmb promoter R	CCCATTCAAACCAAACCAAA
Olfm4 promoter F	TTCAGTTCTGCCTTGGCTCT

Olfm4 promoter R	TCTCAGCAACTCCCTCACCT
Tnfrsf19 promoter F	TAAGGTGGCGATTTCTCAGC
Tnfrsf19 promoter R	ATGCCTTCCTTCTGAGTTGC
Control F	TTGTCTCCCTCTCGGTGAGT
Control R	CTCTGCACTGAAAGGCTGTG

Supplemental References

Carpenter, B., McKay, M., Dundas, S.R., Lawrie, L.C., Telfer, C., and Murray, G.I. (2006). Heterogeneous nuclear ribonucleoprotein K is over expressed, aberrantly localised and is associated with poor prognosis in colorectal cancer. British journal of cancer *95*, 921-927.

Coghlin, C., Carpenter, B., Dundas, S.R., Lawrie, L.C., Telfer, C., and Murray, G.I. (2006). Characterization and over-expression of chaperonin t-complex proteins in colorectal cancer. The Journal of Pathology *210*, 351-357.

Duncan, R., Carpenter, B., Main, L.C., Telfer, C., and Murray, G.I. (2008). Characterisation and protein expression profiling of annexins in colorectal cancer. British journal of cancer *98*, 426-433.

Emmenlauer, M., Ronneberger, O., Ponti, A., Schwarb, P., Griffa, A., Filippi, A., Nitschke, R., Driever, W., and Burkhardt, H. (2009). XuvTools: free, fast and reliable stitching of large 3D datasets. J Microsc *233*, 42-60.

Hope, N.R., and Murray, G.I. (2011). The expression profile of RNA-binding proteins in primary and metastatic colorectal cancer: relationship of heterogeneous nuclear ribonucleoproteins with prognosis. Human pathology *42*, 393-402.

Kumarakulasingham, M., Rooney, P.H., Dundas, S.R., Telfer, C., Melvin, W.T., Curran, S., and Murray, G.I. (2005). Cytochrome p450 profile of colorectal cancer: identification of markers of prognosis. Clinical cancer research : an official journal of the American Association for Cancer Research *11*, 3758-3765.

Novak, A., Guo, C., Yang, W., Nagy, A., and Lobe, C.G. (2000). Z/EG, a double reporter mouse line that expresses enhanced green fluorescent protein upon Cre-mediated excision. Genesis *28*, 147-155.

O'Dwyer, D., Ralton, L.D., O'Shea, A., and Murray, G.I. (2011). The proteomics of colorectal cancer: identification of a protein signature associated with prognosis. PLoS One *6*, e27718.

Sato, T., Vries, R.G., Snippert, H.J., van de Wetering, M., Barker, N., Stange, D.E., van Es, J.H., Abo, A., Kujala, P., Peters, P.J.*, et al.* (2009). Single Lgr5 stem cells build crypt-villus structures in vitro without a mesenchymal niche. Nature *459*, 262-265.